Research Article

Removal of Cationic Textile Dye (C.I. Number 11105) from Aqueous Solution by Adsorption on to Prepared Activated Carbon

T. V. Nagalakshmi[1*], K.A. Emmanuel[2], Ch. Suresh Babu[3] and Ch. Chakrapani[4]

[1]Department of chemistry, Acharya Nagarjuna University, Nagarjuna nagar, Guntur-522510, A.P., India
[2]Department of Chemistry, Sir C R Reddy Autonomous College, Eluru-534 007, A.P., India
[3]Department of Science & Humanities, Eluru College of Engineering & Technology, Eluru-534004, A.P., India
[4]Department of Basic science & Humanities, Gudlavalleru Engineering College, Gudlavalleru-521356, A.P., India

Abstract

Activated carbon adsorbent was prepared from jackfruit waste and named as JC_{HNO3}.Batch sorption experiments were carried out with JC_{HNO3} for the removal of cationic dye Basic Blue 41(BB41) from its aqueous solution. The effect of adsorbent mass, particle size, solution P^H contact time and initial dye concentration were studied. It has been found that, solution P^H greatly influence sorption process JC_{HNO3} was characterized by BET, SEM and FTIR analyses. The BET surface area of JC_{HNO3} was found to be $987 m^2 g^{-1}$. The Frendlich, Langmuir, Tempkin and Dubinin-Radushkerich (D-R) Isotherms were used to describe adsorption equilibrium. The results indicated that Langmur Isotherm was best suited. The kinetics of adsorption process was examined using pseudo-first order, Pseudo- second order, Intra particle diffusion, pore distribution and Elovich models. The adsorption process can be best described by pseudo-second order model.

Keywords: Adsorption, Basic Blue41, SEM, Isotherms, kinetics.

***Correspondence**
Author: T. V. Nagalakshmi
Email: mannava_laxmi@yahoo.co.in

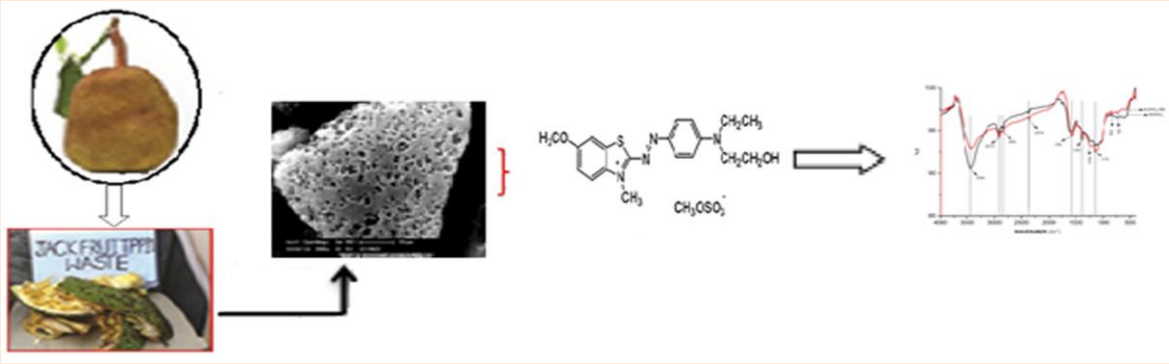

Introduction

Textile dyes have complex aromatic molecular structures. If untreated textile effluents are discharged to near-by water bodies, those molecular structures behave inert and do not bio-degradable [1]. Different types of conventional waste water treatments like coagulation, flocculation, filtration, oxidation (or) reduction and complex formations are costly textile effluent treatment process [2]. Adsorption of these dyes on to activated carbon is the one of the key technique to get clean water. As commercial activated carbon was expensive, researches are showing interest to find alternate sources like Pine cone [3], Coaca shell [4] Pomegranate peel [5], Coconut shell [6], Rice husk [7] for preparation of low cost activated carbons.

In 2012 Asia-Pacific Association of Agricultural Research Institutions (APAARI) stated that, the cultivation land for Jackfruit in India was more than in one lakh hectares [8]. The waste produced from this fruit, if not properly dispose, it leads to pollution. So in the present study Jackfruit pechiparai-1 waste was selected to prepare activated carbon and is efficiency in removing Basic Blue 41 dye from aqueous solution was tested.

Material and Methods

Preparation of activated carbon

Jackfruit of *pichiparai*-1 variety was selected; its rind and pulp waste was washed with hot distilled water to remove dirt and dehydrated at 105ºC until constant weight was obtained. This dried waste was then cut into small pieces and was mixed with K_2CO_3 solution at impregnation ratio 1. Impregnation ratio (IR) was given by weight of K_2CO_3 (g) in solution/weight of waste in g. It was dehydrated in an oven overnight at 105ºC. The impregnated material was carbonized in uniform nitrogen flow at 600ºC. The heating was provided at rate of 10ºC min^{-1} from room temperature. The prepared carbon was cooled to room temperature and washed with hot distilled water to remove remaining chemical and filtered. The washing and filtration steps were repeated until the filtrate showed neutral pH. The activated carbon was sieved to 150, 90, 75 and 45mesh. They were subjected to liquid phase oxidation with 0.1N HNO_3 for 3hours individually. The filtered carbons were washed with distilled water until filtrate showed neutral pH. They were dehydrated in an oven overnight at 105ºC. Activated carbon having 45mesh size was used in sorption processes and named as 'JC_{HNO3}'. And other carbons with 150, 90 and 75mesh were only used to study the effect of particle size.

Preparation of Adsorbate

All reagents used in this study are of analytical grade. The cationic textile dye, BB41, used in this experiment was supplied by SIGMA ALDRICH. It is directly taken to prepare stock solution without further purification. Stock solution (1000 mg l^{-1}) of dye was prepared by dissolving 1g dye into one liter double distilled water. The structure of the BB41 was shown in **Figure 1**.

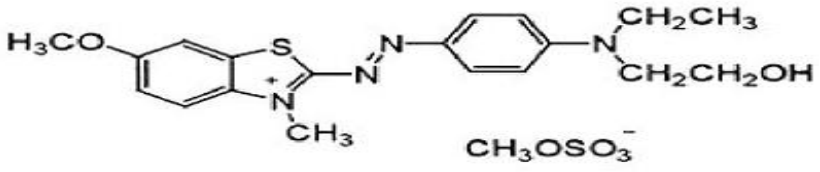

Figure 1 Molecular structure of Basic Blue 41

Determination of zero point charge (pHzpc)

Zero point charge is the pH at which the external surface charge is zero [9]. 50 cm^3 of 0.01 M NaCl solution was placed in a closed Erlenmeyer flask. The pH was adjusted to a value between 2 and 12 by adding 0.1N HCl or NaOH solutions. Then, 0.15 g of carbon sample was added and the final pH measured after 48 h under agitation at room temperature. The pH*zpc* is the point where the curve pH (final) vs. pH (initial) crosses the line pH (final) = pH(initial) taken as the pH_{ZPC} of the given carbon [10].

BET surface area

The pore structure characteristics of prepared carbons were determined by nitrogen adsorption at −196ºC by a Quanta chrome instrument (Nova 2200). Prior to gas adsorption measurements, the carbon was degassed at 150ºC in a vacuum condition for 24 h. Nitrogen adsorption isotherms were measured over a relative pressure (P/P_o) range from approximately 0.03 to 0.995. The BET surface area was determined by means of the standard BET equation applied in the relative pressure range from 0.06 to 0.3.

SEM analysis

A scanning electron microscope SEM Hitachi- S520 (OXFORD LINK-ISIS) was used to study the texture of the surface of JC_{HNO3}, before and after dye adsorption.

FTIR analysis

The surface chemistry characterization of JC_{HNO3}, before and after dye adsorption, was performed Fourier Transform

Infrared Spectroscopy (FTIR) to identify its surface functional groups. FTIR spectra were recorded on Thermo Nicolet Nexus 670 spectrometer in the wave number range 400–4000 cm^{-1}.

Batch adsorption studies

All experiments were carried out in 250 ml conical flasks with 100 ml test solution at room temperature (25±2°C). The flasks, along with test solution and 0.5g of the adsorbent for BB41 at neutral pH, were shaken in horizontal shaker at 120 rpm to study the equilibration time (10-100 min) for maximum adsorption of dye and to know the kinetics of adsorption process. At the end of the desired contact time, the samples were filtered using Whatman no. 42 filter paper and filtrates were analyzed for residual dye concentration at wavelength of 617 nm.
Test solution of dye of 50 mg l^{-1} concentration was prepared from fresh stock solution. All the experiments were carried out in 250 ml conical flasks with 100 ml test solution at room temperature (25±2^{0}C). These flasks, along with test solution and adsorbent, were shaken in horizontal shaker at 120 rpm to study the various control parameters. At the end of desired contact time, the conical flasks were removed from shaker and allowed to stand for 2 min for settling the adsorbent. The adsorbent and dye solution were separated using filtration method. The samples were filtered using Whatman no. 42 filter paper, the first part of the filtrate was discharged to avoid the effects of adsorption on to the filter paper and the remaining filtrate was analyzed for residual dye concentration using UV-visible spectrophotometer. To correct any adsorption of dye on containers, control experiments were carried out in duplicate.

$$\%\ removal = \frac{(C_i - C_e)}{C_i} X100 \ldots\ldots\ldots\ldots\ldots (1)$$

$$Amount\ adsorbed\ (q_e) = \frac{(C_i - C_e)}{m} V \ldots\ldots\ldots\ldots\ldots (2)$$

Where C_i = initial concentration of dye solution in mg l^{-1}, C_e = equilibrium concentration of dye solution in mg l^{-1}, m = mass of the adsorbent in grams (g), V = Volume of test solution in liters (l)

Effect of adsorbent dosage

The percentage removal of BB41 by adsorption onto JC_{HNO3} in the range 0.1 to 1g with 50 mg l^{-1} initial concentration of dye and agitation time of 60 min at pH 7 and at temperature (25±2^{0}C) was studied. The results are presented as percentage removal of dye versus adsorbent dosage in **Figure 2**.

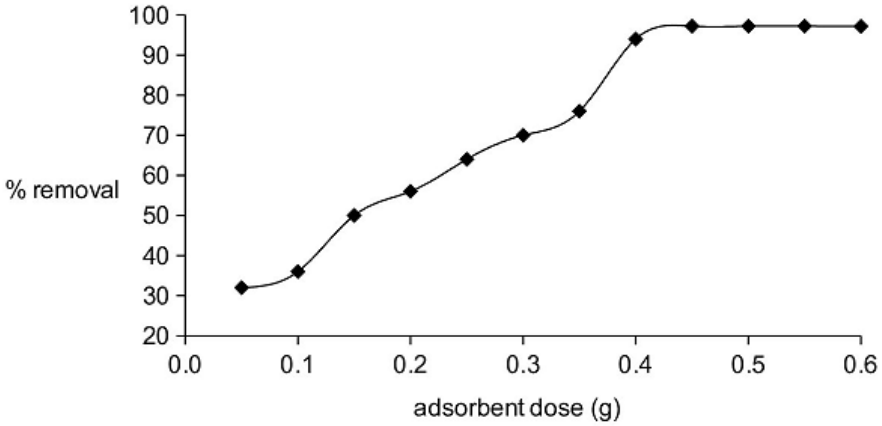

Figure 2 Effect of adsorbent dose on adsorption of BB41 on JC_{HNO3}

Effect of contact time

In order to study the effect of contact time which is related to kinetics of adsorption of dye by JC_{HNO3}, the adsorption

experiments have been conducted in the extent of removal of dye at an optimum initial concentration of dye of 50 mg l^{-1} with optimum dose (0.5g) of adsorbent at pH 7 and at room temperature (25±2°C) by varying the agitation time from 5 to 60 min.The time profile of adsorption of dye onto adsorbent is presented in **Figure 3**.

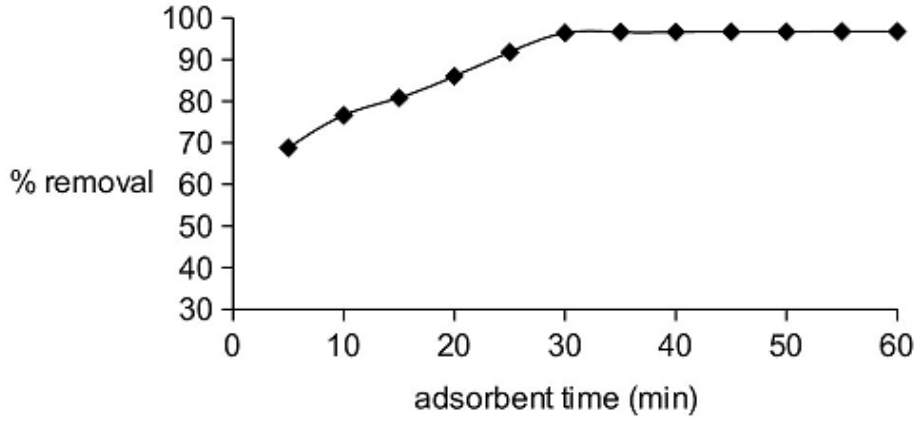

Figure 3 Effect of contact time on adsorption of BB41 on JC_{HNO3}

Effect of initial concentration of dye

The effect of initial concentration of dye on the extent of removal of dye in terms of percent removal and amount of the dye adsorbed on prepared JC_{HNO3} has been studied by varying the initial concentration of dye (range: 10 – 120 mg l^{-1}) and keeping the other control parameters at their optimum conditions. The effect of initial concentration of BB41on adsorption was is shown in **Figure 4**.

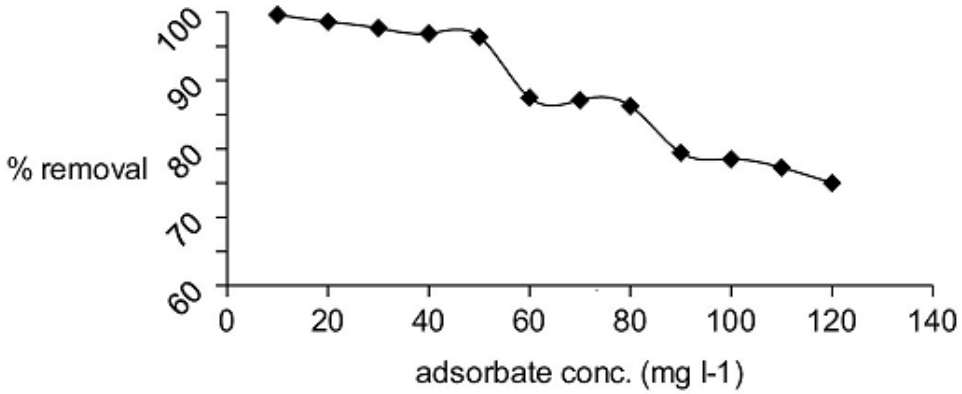

Figure 4 Effect of initial concentration of dye solution on adsorption of BB41

Effect of particle size

To evaluate the influence of the particle size of the adsorbent on the removal of BB41, experiments were conducted with JC_{HNO3} (0.5g) having particle size below 45, 75, 90 and 150 μ at an initial concentration of 50 mg l^{-1} of adsorbate solution with equilibrium time 40 min, at pH 7 and at temperature 25±2°C. The observations were presented in the form a graph in **Figure 5**.

Effect of pH

The effect of pH on adsorption was studied by varying the pH from 3 to 11 under constant process parameters i.e., the initial concentration of the standard dye solution which is 50 mg l^{-1}, the dose of adsorbent is 0.5 g and contact time of 40 min and at room temperature (25±2°C). The results were depicted in **Figure 6**.

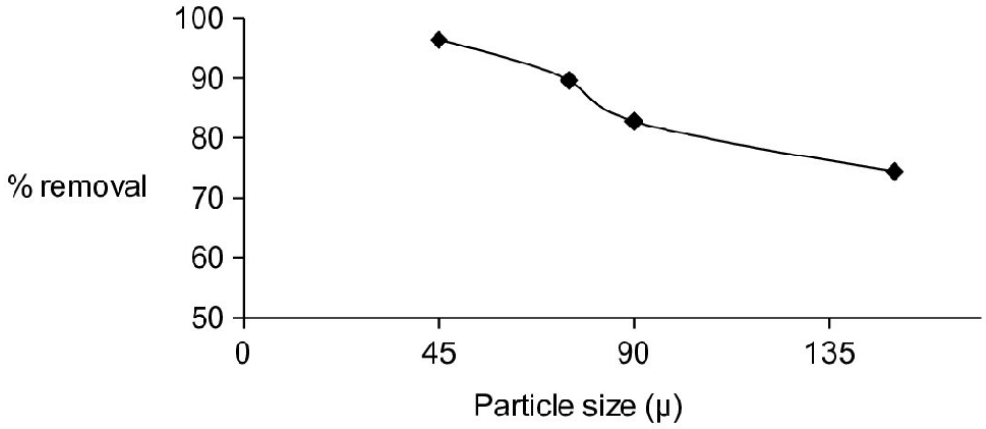

Figure 5 Effect of particle size on adsorption of BB41

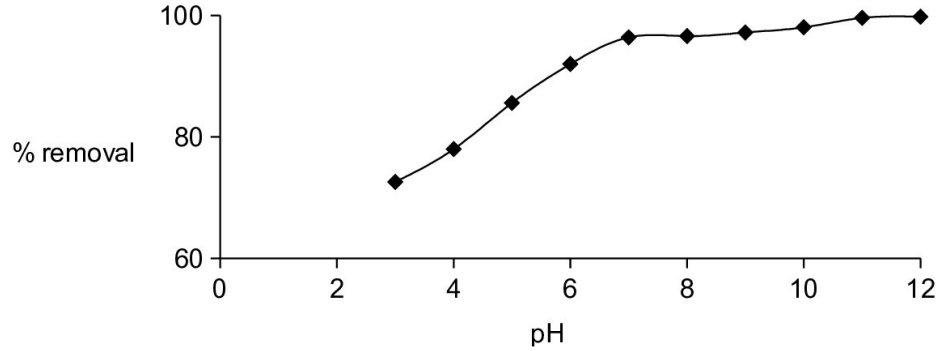

Figure 6 Effect of pH on adsorption of BB41 on JC_{HNO3}

Adsorption isotherms

The experimental data obtained in the present work was tested with the Freundlich [11], Langmuir [12] Tempkin [13] and Dubinin-Radushkevich (D-R) [14] isotherms and the corresponding data is given in **Table 1**.

Chi-square analysis

To identify the suitable isotherm for sorption of dye onto carbon adsorbents, the chi-square analysis was carried out. The mathematical statement for chi-square analysis is

$$\chi^2 = \sum \frac{(q_{e(expt.)} - q_{e(cal.)})^2}{q_{e(expt.)}} \ldots\ldots\ldots\ldots\ldots\ldots (3)$$

Where $q_{e(expt.)}$ and q_e(cal.) are the experimental sorption capacity of dye (mg g^{-1}) at equilibrium time and the corresponding value that is obtained from the sorption model. If data from the model are similar to the experimental data, χ^2 will be a small number, while if they differ; χ^2 will be a bigger number [15].

Adsorption kinetics

To study the adsorption kinetics five kinetic models were used which include pseudo-first-order [16] pseudo-second-order [17], Weber and Morris intraparticle diffusion [18], Bangham's pore diffusion [19] and Elovich models [20]. The relevant equations and results are tabulated in **Table 2**.

Table 1 Isotherms of adsorption of BB41 on JC_{HNO3}

Freundlich adsorption isotherm parameters									
Equation	Graph	R^2	$logk_F$	1/n	k_F	n	$q_{e(expt.)}$	$q_{e(cal.)}$	$\chi 2$
$q_e = k_F C_e^{1/n}$ $logq_e = 1/n\ logC_e + logk_F$	$logq_e$ vs $logC_e$				$mg^{1-1/n}\ l^{1/n}\ g^{-1}$	$g\ l^{-1}$	$mg\ g^{-1}$	$mg\ g^{-1}$	
y=0.3146x+0.7956		0.9730	0.7955	0.3146	6.2445	3.1786	9.64	7.512919	0.469344
Langmuir adsorption isotherm parameters									
Equation	Graph	R^2	a_L/k_L	$1/k_L$	q_m	R_L	$q_{e(expt.)}$	$q_{e(cal.)}$	$\chi 2$
$q_e = k_L C_e/(1+a_L C_e)$ $C_e/q_e = a_L/k_L\ C_e + 1/k_L$	C_e/q_e vs Ce				$mg\ g^{-1}$		$mg\ g^{-1}$	$mg\ g^{-1}$	
Y=0.0567x+0.1040		0.9817	0.0567	0.1040	17.6367	0.2684	9.64	8.7352588	0.08491
Temkin adsorption isotherms parameters									
Equation	Graph	R^2	B	Bln(A)	B	A	$q_{e(expt.)}$	$q_{e(cal.)}$	$\chi 2$
$q_e = RT/bln(Ac_e)$ $q_e = Bln(C_e) + Bln(A)$ *where* $RT/b = B$	q_e vs lnC_e				$kJ\ g^{-1}$	$l\ g^{-1}$	$mg\ g^{-1}$	$mg\ g^{-1}$	
Y=2.4156x+7.8351		0.9387	2.4156	7.8351	1026	25.6243	9.64	9.254957	0.015379
Dubinin-Radushkevich adsorption isotherm paprameters									
Equation	Graph	R^2	lnq_m	B	q_m	E	$q_{e(expt.)}$	$q_{e(cal.)}$	$\chi 2$
$q_e = q_m e^{-\beta\varepsilon 2}$ $lnq_e = -\beta\varepsilon^2 + lnq_m$ where $\varepsilon = RT(1+1/C_e)$ $E=1/\sqrt{(2\beta)}$	lnq_e vs ε^2			mol^2J^{-2}	$mg\ g^{-1}$	$kJ\ mol^{-1}$	$mg\ g^{-1}$	$mg\ g^{-1}$	
y=-0.002x-8.9186		0.9833	-8.9186	0.00200	54.13	15.81	9.6400	8.8632	0.0626

R= Gas constant qe(expt.) and qe(cal.) are the experimental sorption capacity of dye
k_F and1/n are Freundlich constants,q_e ($mg\ g^{-1}$) and Ce($mg\ 1^{-1}$) are the amount of adsorbed adsorbate

Fitness of the kinetic models

The best-fit among the kinetic models was assessed by the squared sum of errors (SSE) values. It is assumed that the model which gives the lowest SSE values is the best model for the particular system [21, 22]. The SSE values were calculated by the equation,

$$SSE = \sum \frac{(q_{e(expt.)} - q_{e(cal.)})^2}{q^2_{e(expt.)}} \dots\dots\dots\dots\dots\dots (4)$$

Where $q_{e\ (expt.)}$ and $q_{e\ (cal.)}$ are the experimental sorption capacity of dye (mg g^{-1}) at equilibrium time and the corresponding value that is obtained from the kinetic models.

Results and discussion

The BET surface area of JC_{HNO3} was found to be 987m^2g^{-1}. The study of effect of adsorbent dose found that the optimum amount of JC_{HNO3} for removal of dye was fixed for further analysis. At 0.5g the percentage removal of dye was found to be 97.20%. From Figure 2 it is clear that the rate of removal of dye was found to be increased rapidly with increase of carbon doses and slowed down later. When the dose increased from 0.5-1g.This could be attributed to increasing adsorbent surface area, augmenting the number of adsorption sites available [23].

Table 2 The adsorption kinetics of BB41 on JC_{HNO3}

Pseudo-first-order								
Equation	Graph	R^2	$k_1/2.303$	$\log(q_e)$	k_1	$q_{e(cal.)}$	$q_{e(expt.)}$	SSE
$dq_t/dt = k_1(q_e-q_t)$ $\log(q_e-q_t) = - k_1t/2.303 + \log q_e$	$\log(q_e-q_t)$ vs t					mg g^{-1}	mg g^{-1}	
y=-0.0367x+0.6729		0.9384	0.0367	0.6729	0.08452	4.7087	9.6400	0.261678945
Pseudo-second-order								
Equation	Graph	R^2	$1/q_e$	$1/(k_2q_e^2)$	k_2	$q_{e(cal.)}$	$q_{e(expt.)}$	SSE
$1/(q_e-q_t) = k_2t + 1/q_e$ $t/q_t = (1/q_e)t + 1/(k_2q_e^2)$	t/q_t vs t					mg g^{-1}	mg g^{-1}	
y=0.0974x+0.2953		0.9986	0.0974	0.2953	0.03213	10.2669	9.6400	0.004229047
Intraparticle diffusion								
Equation	Graph	R^2	k_{ip}	C	k_{ip}	$q_{e(cal.)}$	$q_{e(expt.)}$	SSE
$q_t = k_{ip}t^{1/2} + C$	q_t vs $t^{1/2}$					mg g^{-1}	mg g^{-1}	
y=0.8388x+4.9541		0.9920	0.8388	4.9541	0.8388	9.5484	9.6400	9.02894E-05
Pore diffusion								
Equation	Graph	R^2	A	$\log(k_0/(2.303V))$	k_o	$q_{e(cal.)}$	$q_{e(expt.)}$	SSE
$\log\log(C_i/(C_i-q_tm)) = \alpha\log t + \log(k_0/(2.303V))$	$\log\log(Ci/(Ci-qtm))$ vs $\log t$				ml (g l^{-1})$^{-1}$	mg g^{-1}	mg g^{-1}	
Y=0.154x-1.6101		0.9352	0.1540	-1.6101	5.6519	9.1000	9.6400	0.003137859
Elovich equation								
Equation	Graph	R^2	$1/\beta$	$1/\beta \ln(\alpha\beta t)$	α	$q_{e(cal.)}$	$q_{e(expt.)}$	SSE
$q_t = 1/\beta \ln(1+\alpha\beta t)$ $qt = 1/\beta \ln(t) + 1/\beta \ln(\alpha\beta t)$	q_t vs $\ln(t)$					mg g^{-1}	mg g^{-1}	
Y=1.2447x+4.9272		0.9352	1.2447	4.9272	2.1717	9.3516	9.6400	0.000895028

SSE= Squared Sum of Errors

From **Figure 3** it is evident that, as contact time was increased, initially the percentage removals also increase. But after 30min, it gradually approach constant value, denoting attainment of equilibrium, so 30min was fixed as optimum contact time for further. The changes in the rate of removal of dye with time might be due to the fact that initially all adsorbent sites were vacant and the solution concentration gradient was high. Later the dye uptake rate by adsorbent was decreased significantly due to the decrease in available active adsorbent sites. Decreased removal rate, particularly, towards the end of experiment indicates that the possible monolayer adsorption on surface of adsorbent.

In **Figure 4** it was observed that as dye concentration increase the percentage removal of dye was decreased from 99.80 to 73%. It could be explained by the fact that, at low adsorbate concentration, the ratio of surface active sites to total dye is high. Hence dye molecules have more number of available active sites at low concentration. But with the increase in adsorbate concentration, the number of active sites was not enough to adsorb dye molecule dye ions. However at 50mgl^{-1} the percentage removal of dye was 96.40% and it was fixed as optimum concentration of dye solution.

Figure 5 indicated that the percentage removal of dye was decreased with the increasing particle size of JC_{HNO3}. It might be due to the non availability of more surface area in large sized particles. Hence adsorbent material having size below 45µ were only used for adsorption process. The *PZC* value of JC_{HNO3} was found to be 4. It was stated that if P^H >PZC, acidic functionalities will dissociates, releasing protons into the medium and leaving negatively charged surface on carbon [24].

In **Figure 6** it was depicted that the percent removal of dye below its *PZC* value (*PZC* =4) is very low i.e., from 20-50% after that it was going on increasing and reached 99.8% at alkaline P^H 12, at neutral P^H also the percent removal was 96.4% and it was taken as optimum P^H. Since the dye ion is cation and the adsorbent surface got negative charge after its *PZC* value the electrostatic attraction has been increased and as a result the percent removal might have also increased.

Freundlich plot between $\log q_e$ and $\log c_e$ that show in **Figure 7**(a).The values of K_f and 1/n were obtained from the slop and intercept of the linear plot and were listed in Table 1. Freundlich correlated co-efficient was 0.973. This correlation co-efficient was seemed to be more, the $\chi 2$value was high (0.469). The high $\chi 2$ value indicates that this model was not suitable to explain the sorption process [25].

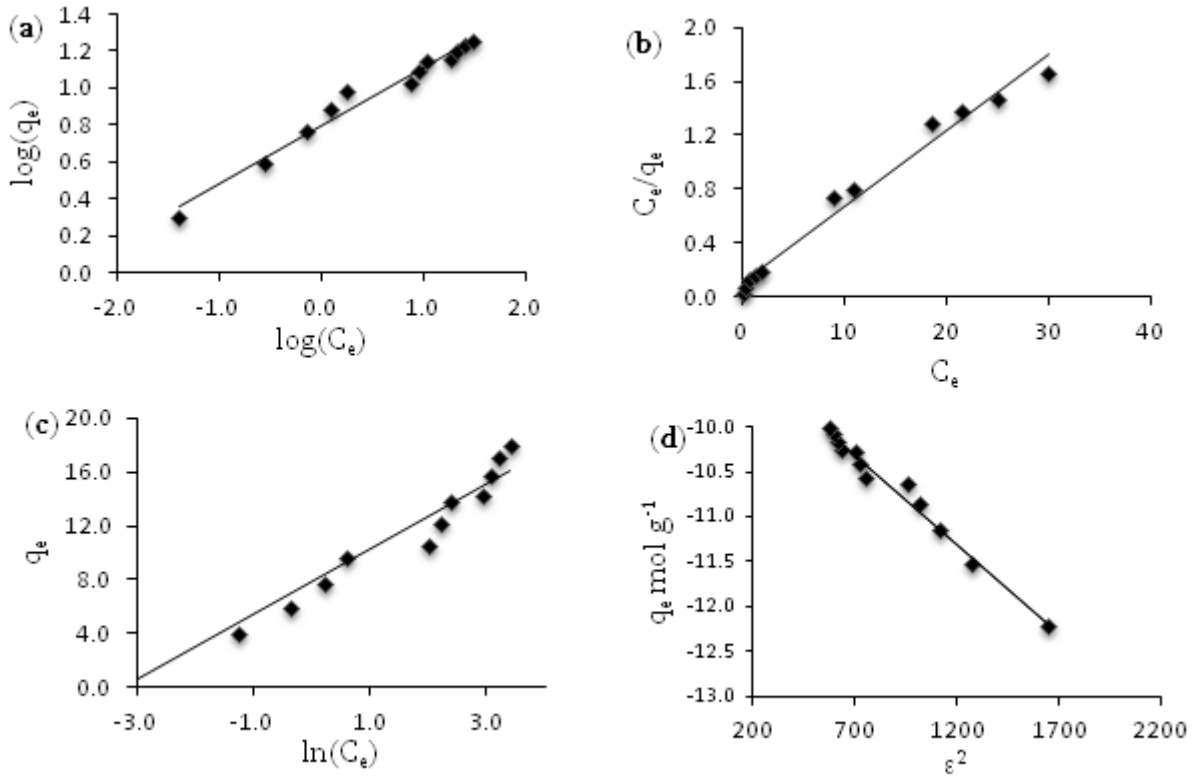

Figure 7 Adsorption Isotherms of BB41 on JC_{HNO_3}.

The Langmuir plot of C_e/q_e as function of C_e was shown in **Figure 7**(b). The values of monolayer capacity (q_m) and Langmuir constant (a_L) were evaluated from the intercept and slope of the plot and were given in Table 1. In comparison with Freundlich isotherm, Langmuir model best fits to explain adsorption phenomenon with its high R^2 value (0.9817) and low $\chi 2$value (0.08491). It was observed that the value of dimensionless constant separation factor (R_L) was 0.2684 (Table-1). Since the value is the range of 0-1 it confirms the favorable uptake of the dye process [26]. The adsorption capacity q_m was found to be 17.6mg g^{-1}. Best fitting of Langmuir isotherms confirms the monolayeral coverage of the dye on to adsorbent surface and also the homogeneous distribution of active sites on the material. Since Langmuir phenomenon assumes that the surface is homogeneous.

Tempkin plot of $\ln C_e$ vs q_e were shown in **Figure 7**(c). The slope of the line gives the value of 'B' and intercept values were given in **Table 1**. The R^2 value for this isotherm was found to be low (0.9387). But the low $\chi 2$ value denotes the suitability of this isotherm up to some extend for dye sorption process. This suggests that the heat of adsorption of all dye molecules in the layer decreases linearly with coverage due to adsorbent-adsorbate interactions and adsorption might be characterized by uniform distribution of binding energies [13].

Dubinin-Radushkevich plot of ε^2 vs q_e was shown in **Figure 7**(d). The values of slope β, q_m and mean free energy E were given in **Table 1**. D-R also showed extent fit to sorption process with its high R^2 (0.983) and low $\chi 2$ (0.0626) values. It indicates the applicability of some degree of heterogeneous surface factor. The value of E (15.81) is within the values of ion exchange. It implies that adsorption mechanism of dye on carbon adsorbent could be chemisorptions [27].

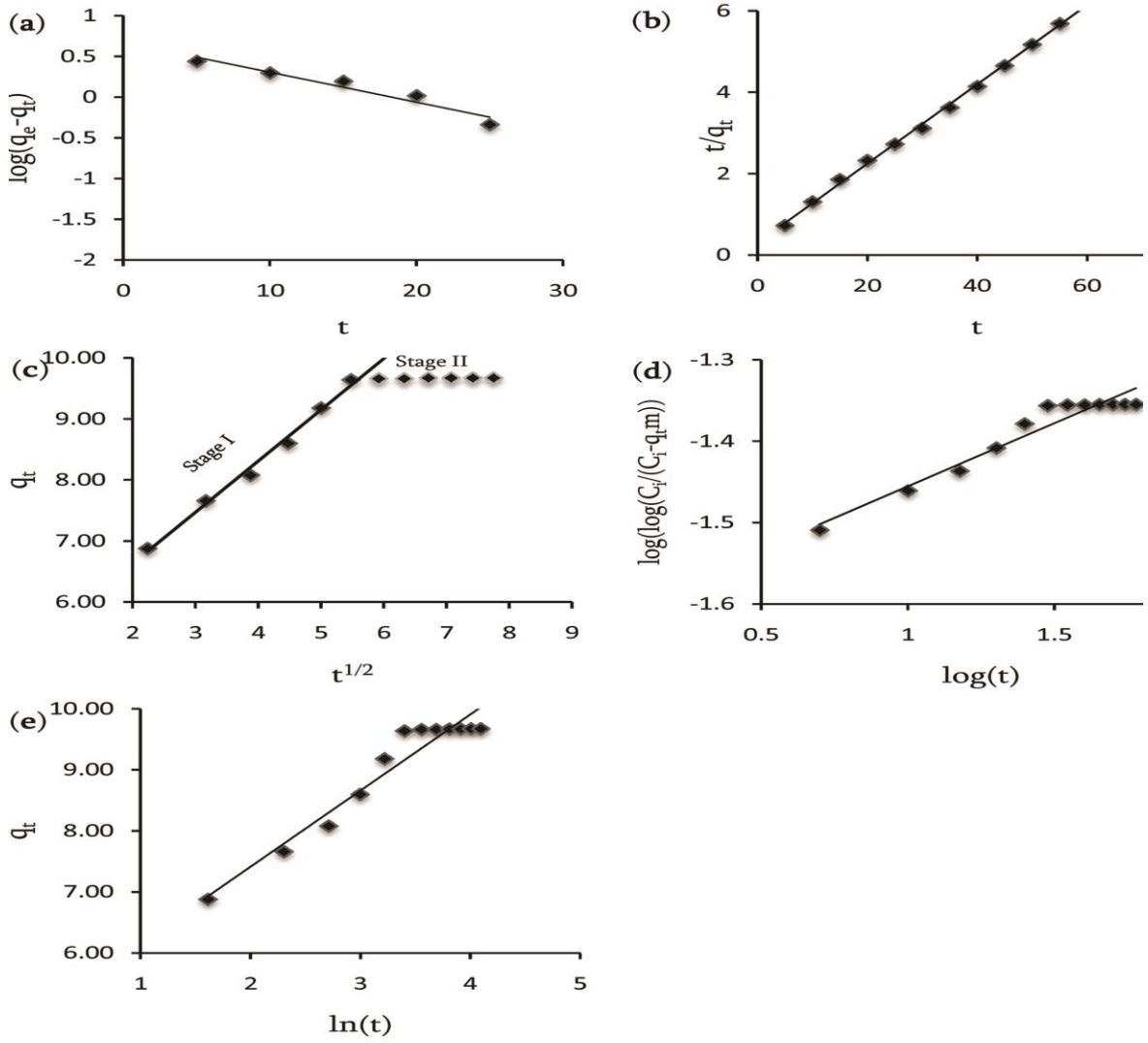

Figure 8. Adsorption Kinetics of BB41 on JC_{HNO_3}

Figure 8(a) represents pseudo first order kinetic model plot of T vs log (q_e-q_t) and corresponding rate constant and R^2 values were given **Table.2**. It has low R^2 (0.9384) and high SSE value (0.262). Not only that log (q_e (expt) [i.e., (log (9.64) =0.984)] is not equal to the intercept value (0.6729) of the plot.This indicates that the sorption kinetics does not follow pseudo-first order kinetics. Figure 8(b) represents pseudo second order kinetic model plot of T vs T/q_t. The slop and intercept values along with R^2 and SSE are given in**Table.2**. It has high R^2value (0.9986) and low SSE value (0.00422). Hence the sorption process can be well described by pseudo -second order model confirming to other well established models. It predicts the behavior over the whole range of studies and it is in agreement with the chemisorptions mechanism being the rate controlling step [28]. **Figure 8**(c) shows intra particle diffusion plots of $t^{1/2}$ vs q_t and corresponding results were tabulating in **Table 2**. It is evident from the plot that there are two separate stages; first linear portion (stage I) and second curved path followed by a plateau (stage II). In stage I j attributed to the immediate utilization of most readily available adsorbing sites on adsorbent surface. In stage –II, very slow diffusion of adsorbate from surface site into the inner pores was observed. So, dye removal mechanism assumed to involve the following 4 steps.

1. Migration of dye from bulk of the solution to the surface of the adsorbent (Bulk diffusion).
2. Diffusion of dye through the boundary layer to the surface of the adsorbent (Film diffusion).
3. Transport of the dye from the surface to the interior pores of the adsorbent (Intra particle diffusion).
4. Adsorption of dye at an active site on the surface of the material (Chemisorption via ion exchange as indicated by the fitting of sorption process to Langmuir and Dubinnin Isotherms).

The intercept of line in Figure 8(c) did not pass through origin. It indicates some degree of boundary layer control in sorption process. So, intra particle diffusion is not only the rate controlling step. Figure 8(d) represents Bangham's plot of log (t) vs log(log(C_i/(C_i-q_t m)) and the corresponding values were tabulated in Table 2. It has moderate R^2 value (0.9352) with low SSE value (0.00314). Therefore the rate determining step of adsorption dye on to adsorbent might be pore diffusion Figure 8(e) represents Elovich plot of *ln (t)* vs q_t and corresponding data were given in Table 2. It also has moderate R^2 value (0.9352) but very low SSE Value (0.00085). Hence adsorption phenomenon also fitted to Elovich Kinetic pattern conformation to this equation alone might be taken as evidence that rate determining step is diffusion in nature [29].And this equation should apply at conditions where rate of desorption can be neglected [30]. **Figure 9** shows SEM image of JC_{HNO3} with more number of pores. These pores were closed by dye molecules which were evidenced by FTIR due to the appearance of new functional groups of dye molecule on dye loaded carbon.

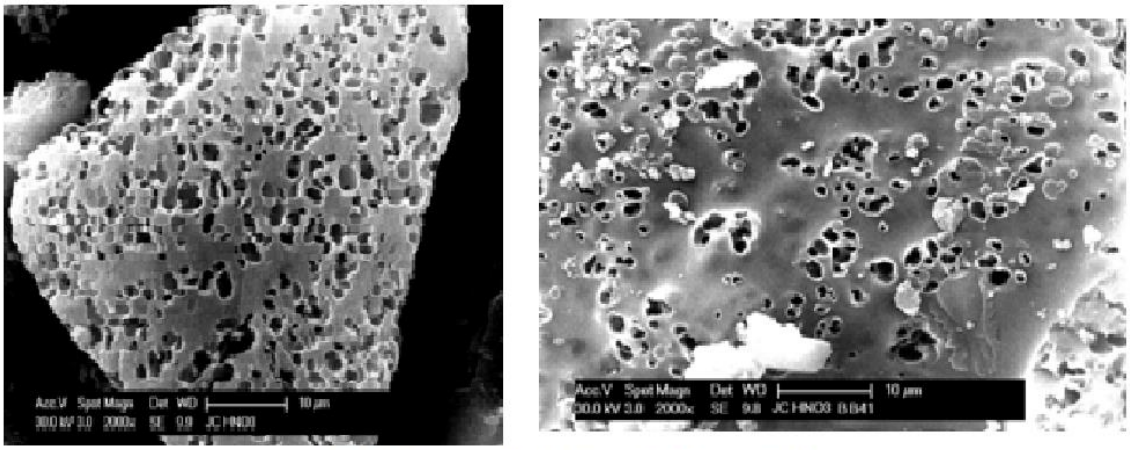

Figure 9 SEM images of (a)JC_{HNO3} (b)JC_{HNO3}-BB41

The FTIR spectra of JC_{HNO3} and $JC_{HNO3\text{-}BB41}$ were shown in **Figure 10**. Bands around 3400-3500 cm^{-1} are due to –OH stretches in hydroxyl, carboxylic and phenolic groups. Bands around 2800-3000 cm^{-1} are due to various C-H stretching modes [31]. Band at 2374 cm^{-1} was attributed to C-H stretching due to presence of CH_2 –CO-group. A distinct peak was observed at 1578 cm^{-1}.This is may be due to poly aromatic C=C stretching vibrations in sp^2-hybridized carbons [32, 33]. In comparison with JC_{HNO3}, the intensity of –OH stretches was decreased in $JC_{HNO3\text{-}BB41}$.

It indicates the possibility of ion-exchange process which was assumed by Dubinin-Radushkevich 'E' value. The intensity of C-H stretching due to presence of CH_2-CO- group was increased in $JC_{HNO3\text{-}BB41}$. It may be due to the presence of carbonyl group present in dye molecule. A distinct peak observed at 1578 cm^{-1} in spectrum of dye loaded carbon is due to the N=N stretching of azo group of BB41.

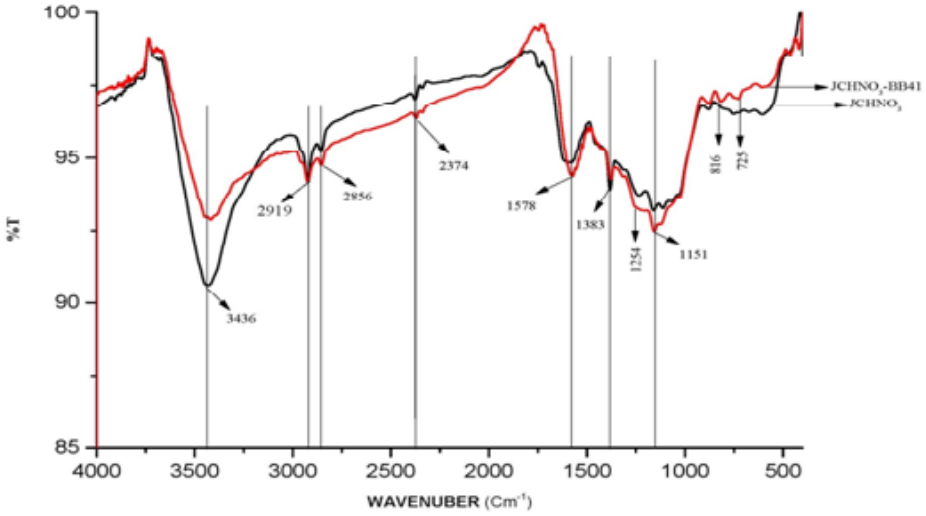

Figure10 FTIR spectrum of JC_{HNO_3} and $JC_{HNO_3\text{-}BB41}$

Conclusion

The prepared JC_{HNO3} successfully removed Basic Blue 41 dye from its 50 mg l^{-1} aqueous solution. The adsorption process reached equilibrium time within 30 min and the required adsorbent dose is 0.5g. The best fit of Langmuir isotherm indicates monolayer adsorption. The kinetics of the process was best described by pseudo second order pattern. It indicates that dye was chemisorbed. However, pore diffusion is one of the rate controlling steps during sorption process.

References

[1] V. A. Shenai, *Colourage*,**1996**, XLIII,41-46.
[2] V. Karthik, K. Saravanan, P. Bharathi, V.Dharanya, C.Meiaraj, *J. Chemical and Pharmaceutical Sciences*, **2014**, 7,301-307.
[3] Mohammad. Bassin Alquaragully, *J. Advanced Research in Chemical Science*, **2014**, 1, 48-59.
[4] Marielen C.Ribas, Matthew A. Adebayo, Lizie D.T. Prola, Eder C. Lima, Renato Cataluña, Liliana A. Feris, M.J. Puchana-Rosero, Fernando M. Machado, Flávio A. Pavan, Tatiana Calvete. *Chemical Engineering Journal*, **2014**, 248, 315-326.
[5] Ahmad, Mohd Azmier, Ahmad Puad, Nur Azreen, Solomon Bello, Olugbenga, *Water Resources and Industry*, **2014**, 6,18–35.
[6] Aseel M. Aljeboree, Abbas N. Alshirifi, Ayad F. Alkaim, *Arabian Journal of Chemistry*, **2014**,doi:10.1016/j.arabjc.2014.01.020
[7] Mohamed. Mokhtar, *Journal of Colloid and Interface Science*, **2004**, 272, 1, 28-34.
[8] APAARI, In: "*Jackfruit improvement in the Asia Pasific region- A status report*", **2012**, 3-4.
[9] H. Marsh, Reinoso.Rodriguez, F. *Elsevier Science & Technology Books*, **2006**, 401-462.
[10] G. Newcombe, R. Hayes, M. Drikas, *Colloids Surf. A*. **1993**, 78, 65-71.
[11] H. Freundlich, *Phys. Chem. Soc*, **1906**, 40, 1361–1368.
[12] I. Langmuir, J. Am. *Chem. Soc*, **1918**, 40, 1361–1368.
[13] M.J. Tempkin, V. V. Pyzhev, *Acta Physiochim*, **1940**, 12, 217–222.
[14] M.M. Dubinin, L.V. Radush Kevich, *Phys. Chem. Sect*. **1947**, 55, 331.

[15] S.K. Lagergren, *Vetenskapsakad. Handl*, **1898**, 24,1–39.
[16] Y.S Ho, G. McKay, *Water Res.* **2000**, 34, 735–742.
[17] W.J. Weber, Jr. J,C. Morris, *J. Sanit. Eng. Div. Am. Soc. Civ. Eng*. **1963**, 89, 31-59.
[18] C. Aharoni, M. Ungarish, *J. Chem. Soc, Faraday Trans*. **1977**, 73, 456–464.
[19] J. Zhang, R. Stanforth, *Langmuir*, **2005**, 21, 2895 – 2901.
[20] S. Meeenakshi, N. Viswanathan, *J. Colloid Interface Sci*, **2007**, 308, 438–450.
[21] S.K,Adhikary, U.K.Tipnis, W.P.Harkare, K.P.Govindan, *Desalination*, **1989**, 71, 301–312.
[22] Y.S. Ho, J.C.Y. Ng, and G. McKay,*Sep. Purif. Methods*, **2000**, 29, 189–232.
[23] K.V. Kumar, K. Porkodi, *J. Hazard. Mater*, **2007**, 146, 214–226.
[24] J.A. Menendez-Diaz, I. Martln-Gullonb, In: Activated Carbon Surfaces in Environmental Remediation, ISBN-13: 978-0-12-370536-5, *Academic press*, **2006**, p. 11.
[25] Pathania. Deepak, Shikha. Sharma, Pardeep. Singh, *Arabian journal of chemistry*.,**2013** doi:10.1016/j.arabjc.2013.04.021
[26] T.W. Weber, R.K. Chakravorti, *J. Am. Inst. Chem. Eng*, **1974**, 20, 228-238.
[27] M.M. Dubinin, *Chem. Rev.*,**1960**, 60, 235–241.
[28] G. McKay, Y.S.Ho, J.C.Y.Ng,*Sep. Purif. Meth*, **1999,** 28, 87–125.
[29] A. Pavlatou, N.A. Polyzopouls, Eur. J. Soil Sci. **1988,** 39, 425–436.
[30] W. Rudzinksi, P. Panczyk, In: J.A. Schwarz, C.I. Contescu (Eds.*), Surfaces of Nanoparticles and Porous Materials*, Dekker, New York,**1998,** p. 355-391.
[31] M. Starsinic, R.L. Taylor, Jr. P.L. Walker, P.C. Painter, *Carbon*, **1983**, 21, 69-74.
[32] P.E. Fanning, M.A. Vannice, *Carbon*, **1993**, 31, 721-730.
[33] E. Papirer, J. Dentzer, S. Li, J.B. Donnet, *Carbon*, **1991,** 29, 69-72.

Publication History
Received 06th Jun 2015
Revised 14th Jun 2015
Accepted 19th Jun 2015
Online 30th Jun 2015